*** Paper for Denali fault earthquake special issue of *Bull. Seism. Soc. Am.* ***
— v. 1.0: 12/30/03 —

Ground motion in Anchorage, Alaska, from the 2002 Denali fault earthquake: Site response and displacement pulses

David M. Boore

Abstract

Data from the 2002 Denali fault earthquake recorded at 26 sites in and near Anchorage, Alaska, show a number of systematic features of importance to studies of site response and in constructing long-period spectra for use in earthquake engineering. The data demonstrate that NEHRP site classes are a useful way of grouping stations according to site amplification. In general, the lower velocity sites have higher amplification. The amplification on NEHRP class D sites reaches a value close to 3, relative to a nearby reference site in the Chugach Mountains. The amplifications are frequency dependent. They are in rough agreement with those from previous studies, but the new data show that the amplifications extend to at least 10 sec, periods longer than considered in previous studies. Beyond about 14 sec all sites have motion of similar amplitude, and the ground displacements are similar in shape, polarization, and amplitude for all stations, particularly if low-passed filtered at a period near 14 sec. The motions at the soil sites are lower than at the reference site for frequencies greater than 8 Hz, with the greatest reduction for the lowest velocity sites (NEHRP class D).

The ground motion is made up of about four pulses, associated with the three sub-events identified in inversion studies (the first pulse is composed of P-waves from the first sub-event). Most of the high-frequency ground-motion is associated with the S-waves from sub-event 1. The pulses from sub-events 1 and 2, with moment releases corresponding to M 7.1 and 6.9, are similar to the pulse of displacement radiated by the M 7.1 Hector Mine earthquake. The signature from the largest sub-event (M=7.6) is more subdued than from

the first two sub-events. The pulses produce response spectra with a peak at a period of about 15 sec. This will be important for engineering considerations of displacement based design.

Introduction

Anchorage, Alaska, is built on a sedimentary basin at the foot of the Chugach Mountains. The city is underlain by thick deposits of Quaternary deposits, including Pleistocene glacial deposits and the silt and clay of the Bootlegger Cove formation (Dutta *et al.*, 2001). Shear-wave velocities, measured at thirty-six sites in the basin (Nath *et al.*, 1997; Dutta *et al.*, 2000), show that most of the city is built on deposits that fall within NEHRP site classes C and D (Figure 1, based on Martirosyan *et al.*, 2002). The combination of the low-velocity sediments and the metamorphic bedrock is an ideal combination for the amplification of seismic waves, and a number of empirical site-amplification studies have been published. These studies include generalized inversion (Dutta *et al.*, 2001) and horizontal-to-vertical spectral ratios (Nath *et al.*, 2002) of weak-motion data from a temporary network of stations. A permanent network of strong- and weak-motion stations was installed after the success of the temporary network. Several studies of site response using weak- and strong-motion recordings from the new network have been published, including the use of spectral ratios (Martirosyan *et al.*, 2002) and generalized inversion (Dutta *et al.*, 2003). These last two studies computed site response at the basin stations relative to a reference site in the nearby Chugach Mountains. All of the studies focused on site response within the 0.5 to 11 Hz frequency range, and not surprisingly, all of the studies found significant frequency-dependent site amplifications on the sediments beneath the city. Although the detailed site-specific findings differ amongst the studies, they all find on average the largest site amplifications on the lower velocity class D sites, with average amplifications around 3 at low frequencies (0.5–2.5 Hz) and around 1.5 at higher frequencies (3.0–7 Hz).

The 2002 **M 7.9** Denali fault earthquake was well recorded on digital strong-motion instruments deployed in the Anchorage metropolitan area. These recordings provide an opportunity to compare site amplifications with those from the earlier studies, which used data from many events, and more importantly, are rich enough in low-frequency content that the site amplifications can be computed at lower frequencies than in the previous

studies. I find that site amplification extends to periods of about 14 sec.

In addition to studies of site amplification, I discuss the pulses of ground displacement on the records. The displacement pulses are similar to those from the much smaller **M** 7.1 Hector Mine, California, earthquake. The pulses are long enough period to be relatively insensitive to local variations in site geology, and they produce a local increase in response spectra at periods between 10 and 20 sec. In addition, the pulses show site-independent but pulse-dependent polarizations. Interestingly, most of the high-frequency content in the ground motion is carried by the *S*-wave pulse produced by sub-event 1. These observations are consistent with the results of Frankel (2004).

Data Processing and Characteristics

The data analyzed in this paper were obtained on force-balance accelerometers whose response is flat to acceleration from 0 Hz to 50 Hz. The sensor output was recorded on dataloggers with 114 db dynamic range at 200 samples per second. The data were provided by the USGS and the University of Alaska and are available from http://nsmp.wr.usgs.gov. The stations are plotted in Figure 1. Almost all data had drifts in displacement derived from double integration of the acceleration trace. To eliminate these drifts, the data were processed using simple baseline corrections and low-cut filtering with a low-order acausal 0.02 Hz Butterworth filter; similar results were obtained using longer period filters.

The three components of ground displacement at two sites underlain by very different materials are shown in Figure 2. The station K2-20 has a strong broad-band site response at about 0.2 Hz, which leads to the increased "chatter" as compared to the recordings at K2-16 (see gray curves in Figure 2). By filtering out high frequencies to eliminate this chatter, it is clear that the longer period motions at these two dissimilar stations are quite similar (see black curves in Figure 2). The displacements are composed of four bursts of energy at times near 35, 70, 100, and 170 sec (these times include pre-event motion, which is of different duration at each station). The first two bursts of energy correspond to the *P*- and *S*-wave arrivals from what has been termed by Frankel (2004) "sub-event 1", corresponding to the thrust fault initiating the earthquake (the Susitna Glacier fault). The second and third bursts of motion correspond to *S*-waves from the strike-slip sub-events 2 and possibly 3 (Frankel, 2004; Eberhart-Phillips *et al.*, 2003). Sub-event 2 was a

concentrated zone of moment release on the portion of the Denali fault near the crossing of the Trans-Alaska Pipeline; sub-event 3 occurred farther east. The moment releases on the three sub-events corresponded to moment magnitudes 7.1, 6.9, and 7.6, respectively (Frankel, 2004).

Hodograms of the horizontal displacements at the two stations K2-20 and K2-16 are shown in Figures 3a and 3b for the four pulses identified in Figure 2. In spite of the difference in higher frequency site response, the polarizations are very similar for the pulses on the two stations (and for the other stations, although not shown here). In fact, the similarity of the polarizations for the stations led me to discover an error in the orientation of the horizontal motion at station K2-16. As confirmed by Dutta (oral communication, 2003), the wrong sign was used for the correction for magnetic declination, resulting in an error of 42.6 degrees. Once I made this correction, the polarizations of K2-16 agreed with those from the other stations.

The polarizations for the first and second pulses are consistent with P- and SH-wave motion from sub-event 1. The clockwise rotation of the polarization from pulses 3 through 4 relative to pulse 2 is consistent with SH-waves being radiated from portions of the Denali fault and Totschunda fault at points progressively to the east of the hypocenter (sub-event 1). Frankel (2004) identifies pulse 2 as coming from sub-event 2. If composed of SH body and surface waves, pulse 3 seems to be coming from an azimuth of about 60 to 70 degrees clockwise from north, which puts its source along the Totschunda fault, to the east of Frankel's sub-event 3. Because his interpretations are based on careful study of a number of records obtained from various locations in Alaska, it is unlikely that sub-event 3 has been mislocated by Frankel (2004). In this case, appeals to lateral refraction to produce rotations of the particle motion can be made, although that seems like special pleading.

Site Response

As indicated in the introduction, a number of previous studies have found significant and systematic site response in the Anchorage area, and therefore it will be no surprise to find the same from records of the Denali fault earthquake. The first indication of site response is in differences of peak acceleration, velocity, and displacements for the various stations. The corresponding time series are shown in Figure 4 for the same two stations

used in the previous figures — K2-20 and K2-16 (the reference station in the Chugach Mountains). As note before, these two stations are underlain by dissimilar near-surface materials. Note the increase of all three measures of ground shaking at K2-20 compared to K2-16, with the greatest difference being for the higher frequency motions. Also seen is something not obvious from plots of peak motions alone: the highest accelerations are associated with pulse 2, with little or no increase of accelerations at the arrival times of pulses 3 and 4 (I show later the influence of this difference on response spectra). This was noted by Frankel (2004) in his interpretation of envelopes of high-frequency ground motions.

Figure 5 shows plots of ratios of peak acceleration, peak velocity, and peak displacement relative to station K2-16, with stations from different site classes indicated by the symbol used in the plot. As measured by the peak motion ratios, the site amplification exists for all three measures of ground motion, but the amplification is clearly more sensitive to site class for peak acceleration than for peak displacement. There are consistent differences in the mean amplifications within each site class, with larger amplifications for lower velocity sites. Much scatter, however, remains for the amplifications within each class, particularly for peak acceleration.

NEHRP classes are also an effective way of grouping the amplifications given both by response spectra (Figure 6) and by Fourier spectra (Figure 7). More information about the periods corresponding to the site amplifications are given by these figures than in the plots of peak ground motions. Although engineers often characterize site response as ratios of response spectra, caution is needed in the interpretation of response spectral amplifications: the oscillator periods do not always correspond to the ground-motion periods, and therefore the site amplification seen in the response spectra do not necessarily correspond to differences of ground motion at the oscillator periods. In the present results this is most dramatically seen for short periods. Recall that the short- and long-period asymptotes of a pseudo-velocity response spectrum are controlled by the peak acceleration and peak displacement of the ground motion used to derive the response spectrum. Note the difference at short periods in the response spectra for the different site classes (Figure 6). These differences are consistent with the peak acceleration ratios shown in Figure 5, as they must be. But they should not be interpreted as indicating greater site amplification at short periods (high frequencies) for lower-velocity sites. In fact, as Figure

7 shows, the opposite is true: there is a deamplification at frequencies greater than 8 Hz (the increase in the ratio around 20 Hz is associated with a hole in the spectrum of the denominator and is not a site effect, at least not one associated with the soil stations). The amplification at lower frequencies is largest for site class D, and the deamplification at higher frequencies is also largest for site class D. This is qualitatively expected as the result of the tradeoff of increased amplification and increased attenuation for the lower velocity materials characterizing class D sites.

Note that the site amplifications extend to periods much longer than used in previous studies of site amplification in Anchorage (the range of the previous studies is shown by the double-sided arrows in Figures 6 and 7). The relatively large radiation at long periods for the Denali fault earthquake makes this possible, and the quantification of site response at long periods is the one thing new to this study.

For periods common both to previous studies and to this study I made quantitative comparisons of the site amplifications. Figure 8 shows a comparison of site amplification from Martirosyan *et al.* (2002) at two stations, relative to K2-16. The amplification has been computed both from Fourier spectra and response spectra. Concentrating only on the Fourier spectra amplification, the comparison is relatively good for station K2-01 in that the frequencies of amplification peaks coincide, as does the general level of amplification. The comparison for K2-02 is not as good, particularly above 2 Hz. Figure 9 shows another comparison, in this case of averages of Fourier spectra over two frequency bands. The amplifications are better for the lower frequency band (0.5–2.5 Hz) than for the higher frequency band (3.0–7.0 Hz), although there is much scatter within each band. It is not surprising to see this scatter, as many studies find significant event-to-event variation for a single station pair and station-to-station variation for a single event (see, e.g., the review by Boore, 2004).

Pulses

One of the interesting features of the recordings in Anchorage are the displacement pulses. This section discusses a few things associated with these pulses: the different frequency content of the pulses, the similarity to pulses from a smaller earthquake occurring in California, and the contribution of the pulses to the long-period response spectral shape.

I noted before that the maximum accelerations are associated with pulse 2. The consequence of this is clearly seen by comparing response spectra for the whole record with those computed for the portions of the records corresponding to the two largest displacement pulses (pulses 2 and 3). The results are shown in Figure 10 for stations K2-2- and K2-16. All of the response at periods shorter than 1 and 4 seconds is contributed by pulse 2 for stations K2-20 and K2-16, respectively, but both pulses contribute essentially equally to the peak in the spectra between 10 and 20 sec. The richness of high-frequency radiation of sub-event 1 (corresponding to pulse 2) relative to sub-events 2 and 3 was noted by Frankel (2004); my results illustrate the same conclusion using a different measure of ground motion.

I was struck with the similarity of the displacement pulses in Anchorage from the **M** 7.9 Denali fault earthquake with the pulse radiated by the **M** 7.1 1999 Hector Mine, California, earthquake (see Boore *et al.*, 2002). To make a quantitative comparison of the pulses, I show in Figure 11 two copies of a representative pulse from the Hector Mine earthquake, after shifting to match the arrival times of the pulses and correcting the amplitudes for differences in propagation distances. The Hector Mine displacement pulse was multiplied by 0.38. This factor was obtained by evaluating the ground-motion prediction equations of Sadigh *et al.* (1997), which were used by Wesson *et al.* (1999) in constructing probabilistic hazard maps for Alaska, with the magnitude of the 1999 earthquake and for distances of 172 km and 320 km (the source-station distance for the 1999 and 2002 earthquakes, respectively). The acceleration times series leading to the displacements were processed in identical ways for both earthquakes (note that the results of Boore *et al.*, 2002, used a causal low-cut filter rather than the acausal low-cut filter used here; the displacement waveforms can be quite different for the two types of filters). The waveforms for the two events are similar, consistent with the finding of Frankel (2004) that pulses 2 and 3 correspond to sub-events of moment magnitude similar to that of the 1999 earthquake (7.1 and 6.9, compared to 7.1 for the Hector Mine earthquake). Although the displacement pulses are similar, close inspection shows that the pulses from the Denali fault earthquake have a somewhat longer duration. This leads to relatively more long-period content in the response spectra (Figure 12). In both cases the peak in response spectra at periods of about 8 and 15 sec is a feature not included in most spectra used for engineering design. Also, in both cases the peak is due to the source and not to local site response. Of course the observation of enhanced source-related long-period peaks in response spectra from only

two earthquakes is not enough to produce a change in schemes for constructing engineering design spectra. It is very likely, however, that more such examples will be found from data recorded by the increasing number of modern broadband digital recorders.

Conclusions

This purely observational study of digital strong-motion data from the 2002 Denali fault earthquake recorded in and near Anchorage, Alaska, finds a number of systematic features of the ground motion. In agreement with previous studies, I find significant ground-motion amplification at soil sites, relative to a nearby reference site in the Chugach Mountains. New to this study is the finding that the site amplification extends to periods of at least 10 sec. I also find a deamplification at frequencies greater than 8 Hz (the deamplifications are not seen in the response spectra because of the nature of response spectra). The amplifications are well differentiated by NEHRP site class, with the class D amplifications, relative to a reference station in the nearby Chugach Mountains, reaching a value near 3.

The ground displacements are made up of a series of pulses, corresponding to the sub-events along the fault identified in source inversion studies (e.g., Frankel, 2004). The two largest pulses are similar in shape and amplitude to the pulse radiated by the 1999 Hector Mine, California earthquake. The moment magnitude of that earthquake (7.1) is similar to the moment magnitudes inferred for sub-events 1 and 2 of the Denali fault earthquake (7.1 and 6.9, respectively [Frankel, 2004]). These pulses produce a localized long-period peak in response spectra, with the peak for the Denali recordings being at a longer period than for the Hector Mine earthquake recordings (about 15 sec vs. 8 sec). The pulses have polarizations that are similar for all stations, and show a systematic clockwise rotation from pulse 2 to pulse 4, consistent with SH-waves radiated from localized source at points along the faulting progressively to the east of the hypocenter. As noted by Frankel (2004), most of the high frequency motion is carried by the S-wave pulse from sub-event 1; the other sub-events apparently radiated relatively little high-frequency energy.

Acknowledgments

I am greatly indebted to Chris Stephens for providing data, insightful conversations,

and a review of the paper. I also thank Art Frankel for some of his results. Reviews by xxx and yy were very helpful.

References

Bommer, J.J. and A.S. Elnashai (1999). Displacement spectra for seismic design, *J. Earthq. Eng.* **3**, 1–32.

Boore, D. M. (2004). Can site response be predicted?, *J. Earthq. Eng.* **8**, (in press).

Boore, D.M., C.D. Stephens, and W.B. Joyner (2002). Comments on baseline correction of digital strong-motion data: Examples from the 1999 Hector Mine, California, earthquake, *Bull. Seism. Soc. Am.* **92**, 1543–1560.

Eberhart-Phillips, D., P. J. Haeussler, J. T., J. T. Freymueller, A. D. Frankel, C. M. Rubin, P. Craw, N. A. Ratchkovski, G. Anderson, G. A. Carver, A. J. Crone, T. E. Dawson, H. Fletcher, R. Hansen, E. L. Harp, R. A. Harris, D. P. Hill, S. Hreinsdóttir, R. W. Jibson, L. M. Jones, R. Kayen, D. K. Keefer, C. F. Larsen, S. C. Moran, S. F. Personius, G. Plafker, B. Sherrod, K. Sieh, N. Sitar, and W. K. Wallace (2003). The 2002 Denali fault earthquake, Alaska: A large magnitude, slip-partitioned event, *Science* **300**, 1113–1118.

Frankel, A. (2004). Rupture process of the **M**7.9 Denali fault, Alaska, earthquake: Subevents, directivity, and scaling of high-frequency ground motions, *Bull. Seism. Soc. Am.* **94**, (submitted).

Dutta, U., N. Biswas, A. Martirosyan, S. Nath, M. Dravinski, A. Papageorgiou, and R. Combellick (2000). Delineation of spatial variation of shear-wave velocity with high frequency Rayleigh wave, *Geophys. J. Int.* **143**, 365–376.

Dutta, U., A. Martirosyan, N. Biswas, A. Papageorgiou, and R. Combellick (2001). Estimation of *S*-wave site response in Anchorage, Alaska, from weak-motion data using generalized inversion method, *Bull. Seism. Soc. Am.* **91**, 335–346.

Dutta, U., N. Biswas, A. Martirosyan, A. Papageorgiou, and S. Kinoshita (2003). Estimation of earthquake source parameters and site response in Anchorage, Alaska from strong-motion network data using generalized inversion method, *Phys. Earth Planet. Inter.* **137**, 13–29.

Martirosyan, A., U. Dutta, N. Biswas, A. Papageorgiou, and R. Combellick (2002). Determination of site response in Anchorage, Alaska, on the basis of spectral ratio methods, *Earthquake Spectra* **18**, 85–104.

Nath, S. K., D. Chatterjee, N. N. Biswas, M. Dravinski, D. A. Cole, A. Papageorgiou, J. A. Rodriguez, and C. J. Poran (1997). Correlation study of shear-wave velocity in near-surface geological formations in Anchorage, Alaska, *Earthquake Spectra* **13**, 55–75.

Nath, S. K., N. N. Biswas, M. Dravinski, and A. S. Papageorgiou (2002), Determination of S-wave site response in Anchorage, Alaska in the 1–9 Hz frequency band, *Pure and Applied Geophy.* **159**, 2673–2698.

Sadigh, K., C.-Y. Chang, J.A. Egan, F. Makdisi, and R.R. Youngs (1997). Attenuation relationships for shallow crustal earthquakes based on California strong motion data, *Seism. Res. Lett.* **68**, 180–189.

Wesson, R. L., A. D. Frankel, C. S. Mueller, and S. C. Harmsen (1999). Probabilistic seismic hazard maps of Alaska, *U.S. Geol. Surv. Open-File Rept. 99-36*, .

Author Affiliation:

U.S. Geological Survey, MS 977
345 Middlefield Road
Menlo Park, CA 94025
boore@usgs.gov

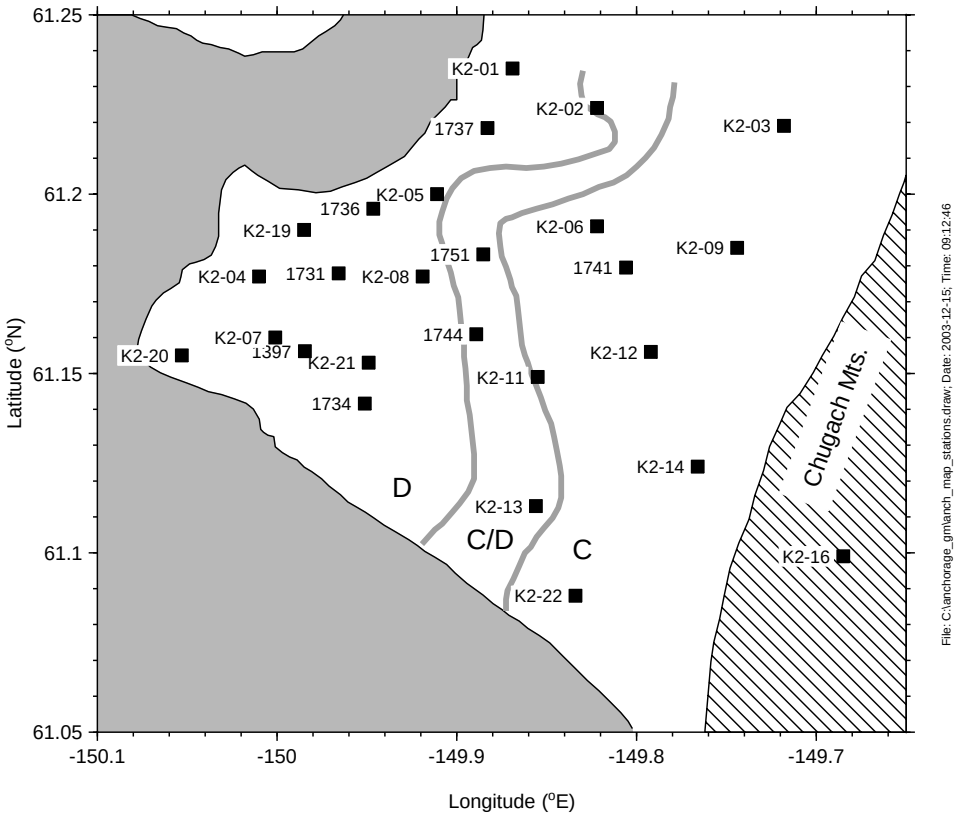

Figure 1. Location of stations and NEHRP site classes (site classes and base map from Figure 12 in Martirosyan *et al.*, 2002). The C/D class is intermediate between NEHRP classes C and D, and is defined by Martirosyan *et al.* (2002) by the average shear wave velocity to 30 m being between 320 and 410 m/sec.

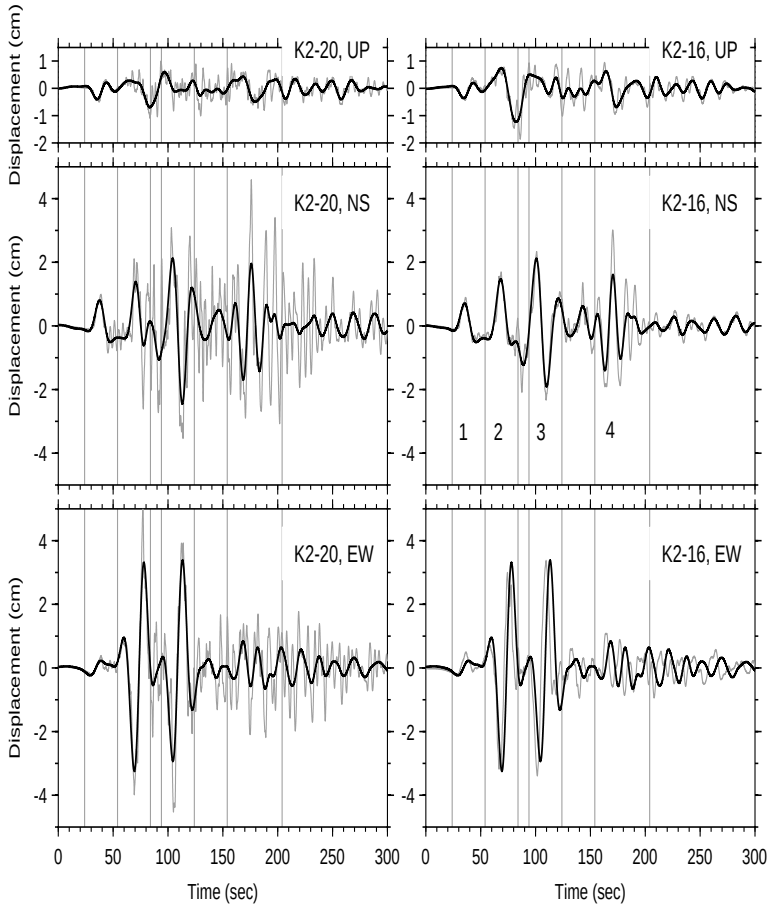

Figure 2. Displacements at stations K2-16 and K2-20, showing the strong (and differing) polarization of the dominant displacement pulses. The gray lines indicate the windows used in constructing hodograms. Station K2-20 is on lower velocity materials and has more high frequency motion than does station K2-16. The numbers below the K2-16, NS trace label the pulses referred to in the text. Gray curves have been low-cut filtered at 0.02 Hz; black curves have also been high-cut filtered at 0.08 Hz.

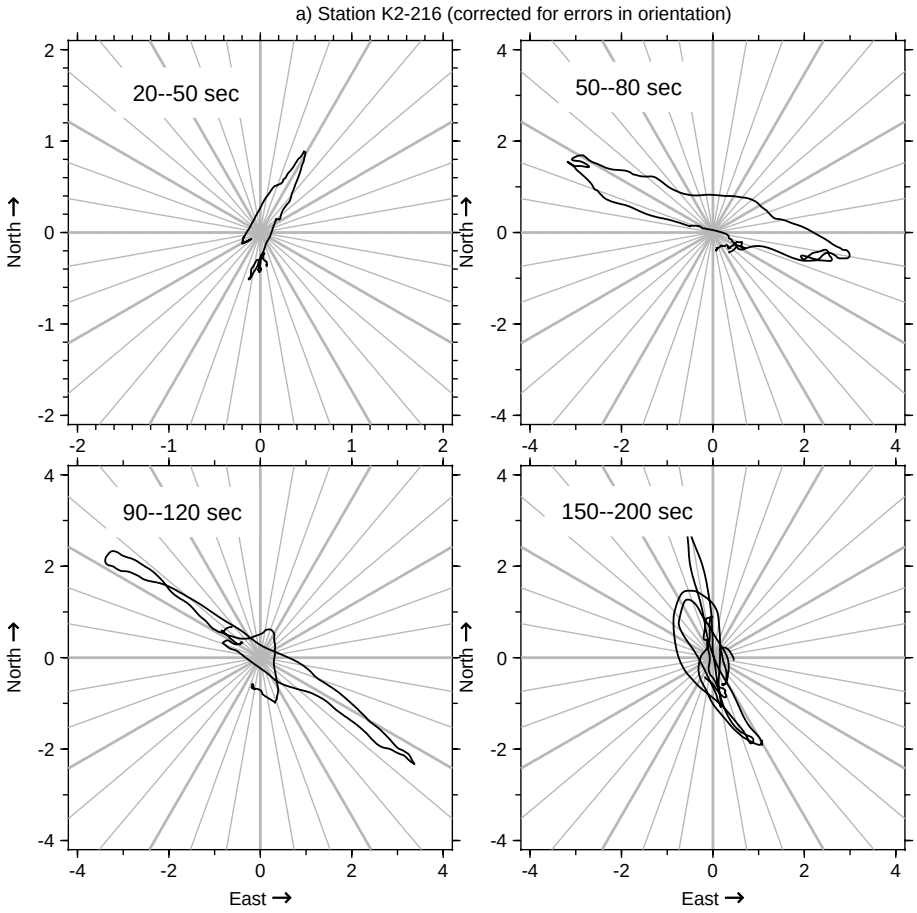

Figure 3a). Hodograms of horizontal displacements at station K2-16 for four time windows (shown on previous figure), showing the strong (and differing) polarization of the dominant displacement pulses. Note that the scale for the graph showing the displacements in the first time window (20–50 sec) is half that of the other graphs.

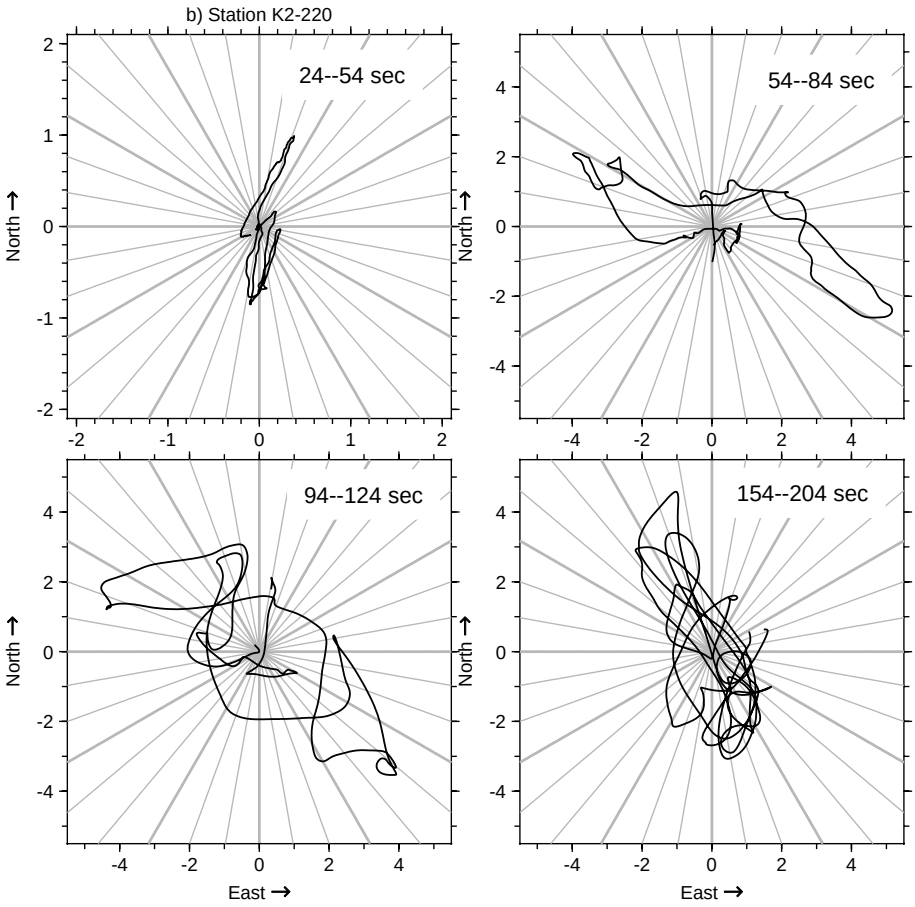

Figure 3b). Hodograms of horizontal displacements at station K2-20 for four time windows (shown on previous figure), showing the strong (and differing) polarization of the dominant displacement pulses. Note that the scale for the graph showing the displacements in the first time window (24–54 sec) is half that of the other graphs.

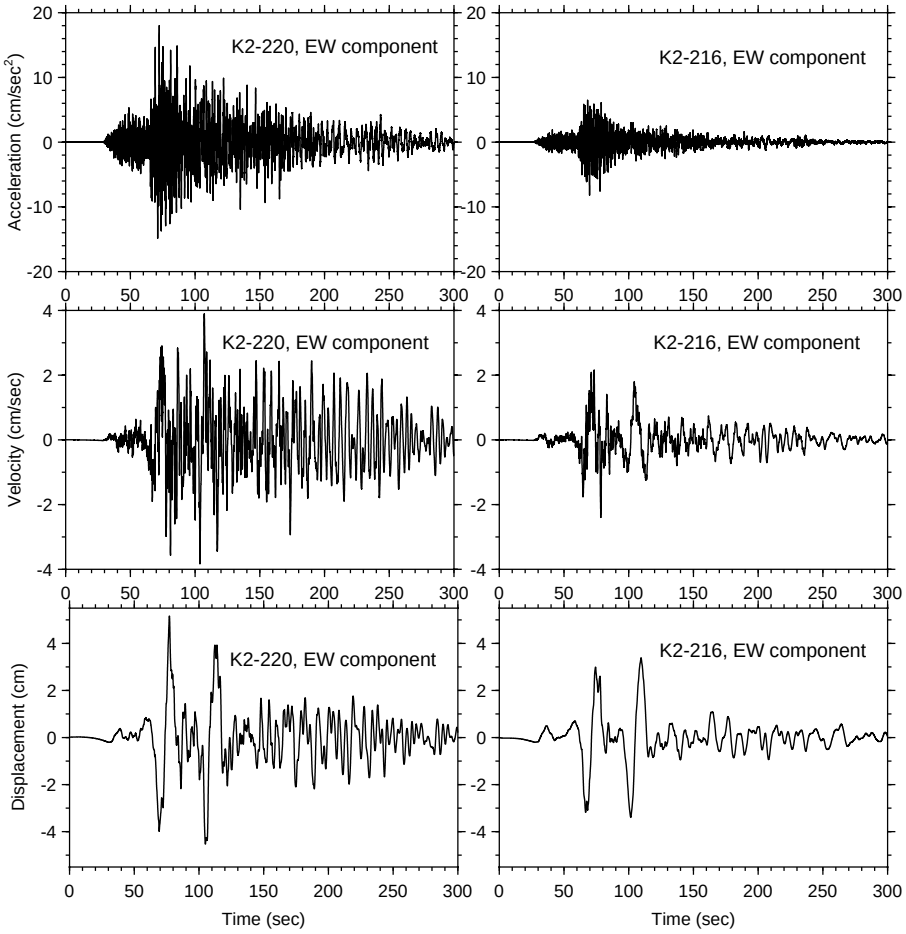

Figure 4. Accelerations, velocities, and displacements at stations K2-20 and K2-16.

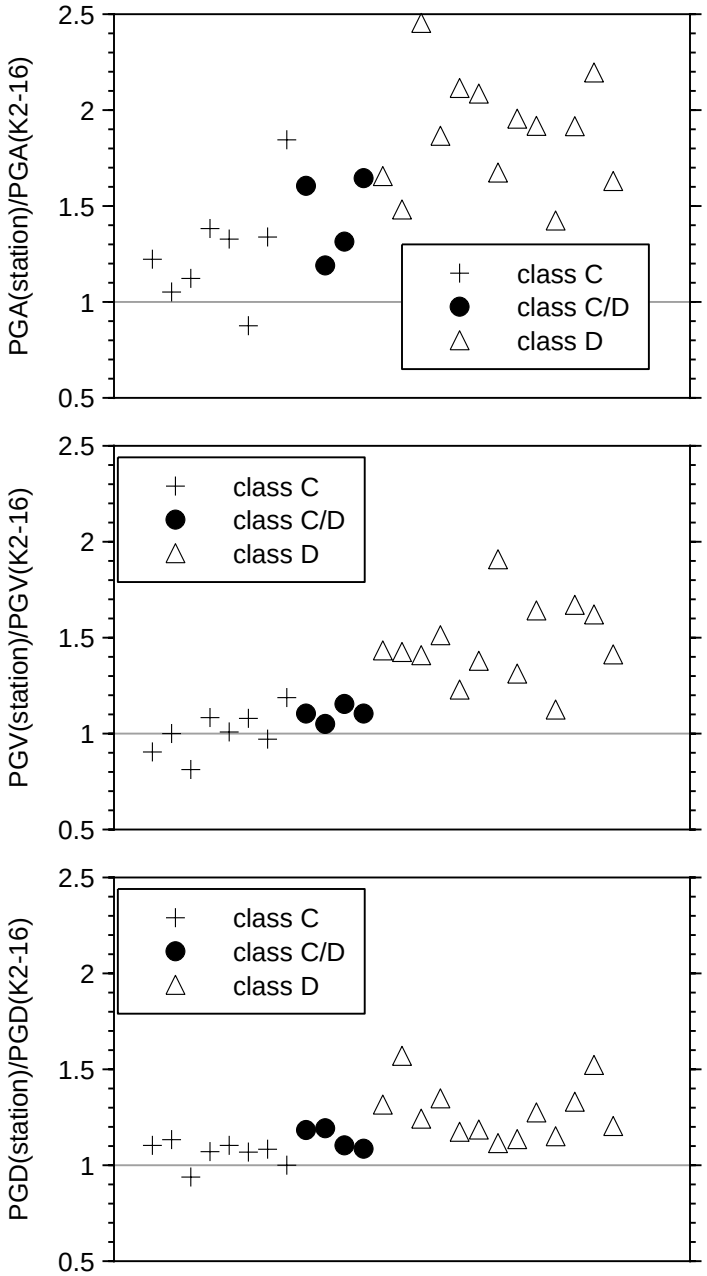

Figure 5. Peak accelerations, velocities, and displacements, relative to station K2-16, grouped by site class. All motions were oriented EW.

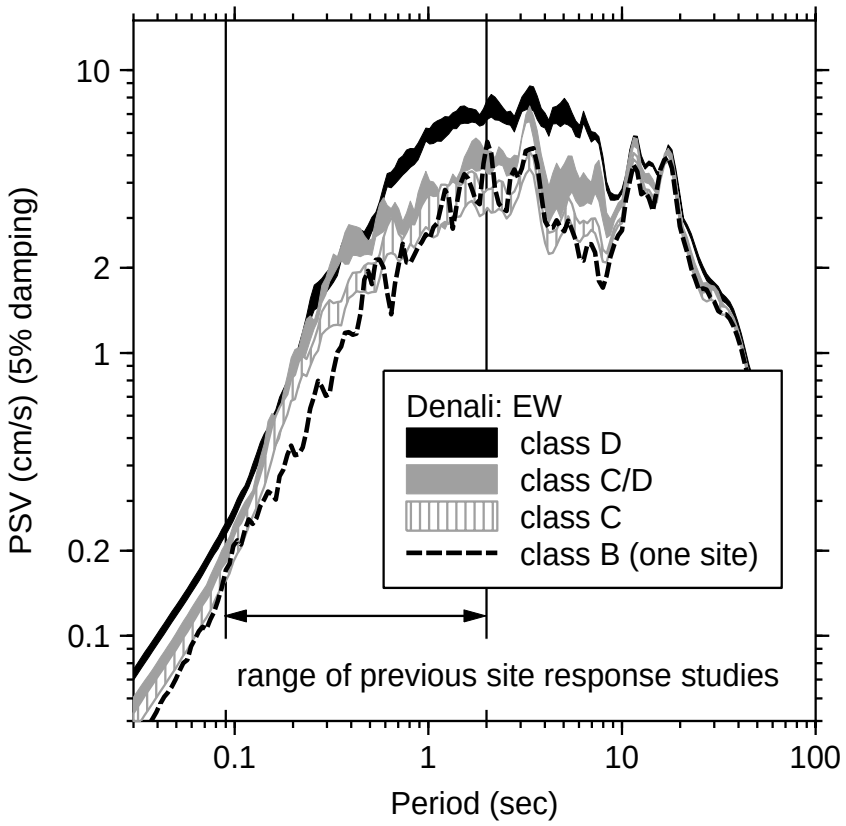

Figure 6. 5%-damped pseudo relative velocity response, showing the range of the standard error of the median by site class.

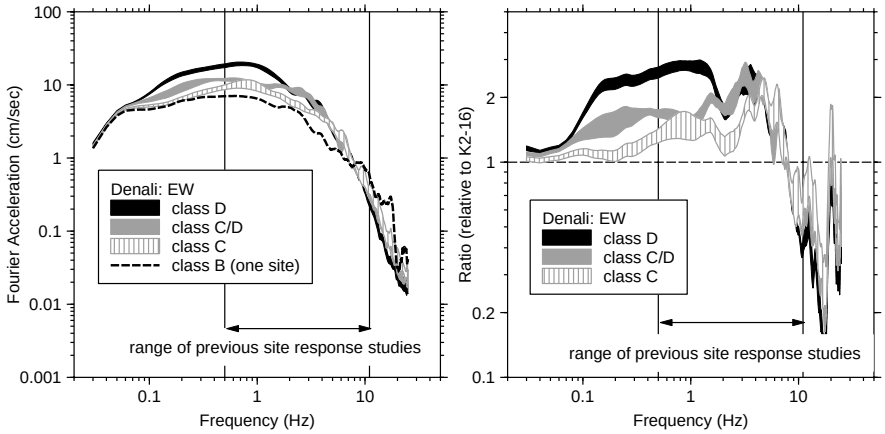

Figure 7. Average of smoothed Fourier amplitude spectra of the east-west motion for recordings on the same NEHRP site class, and ratio of the average spectra relative to the spectrum at K2-16. The individual spectra were smoothed with a triangular smoothing operator with a base width of 1 Hz.

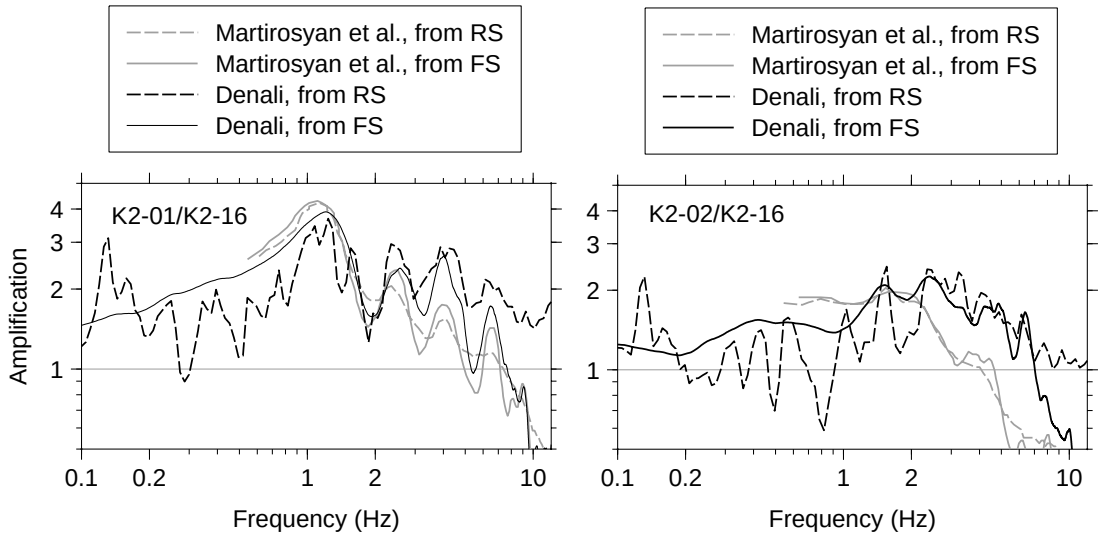

Figure 8. Site response at stations K2-01 and K2-02 computed from Fourier amplitude spectra and response spectra. Shown are the site responses from the Denali earthquake ground motion and from the averages of 46 events, as determined by Martirosyan *et al.* (2002; rms of the two horizontal components). The EW component of motion was used for the Denali earthquake recordings. The Fourier spectra have been smoothed before computing the ratios.

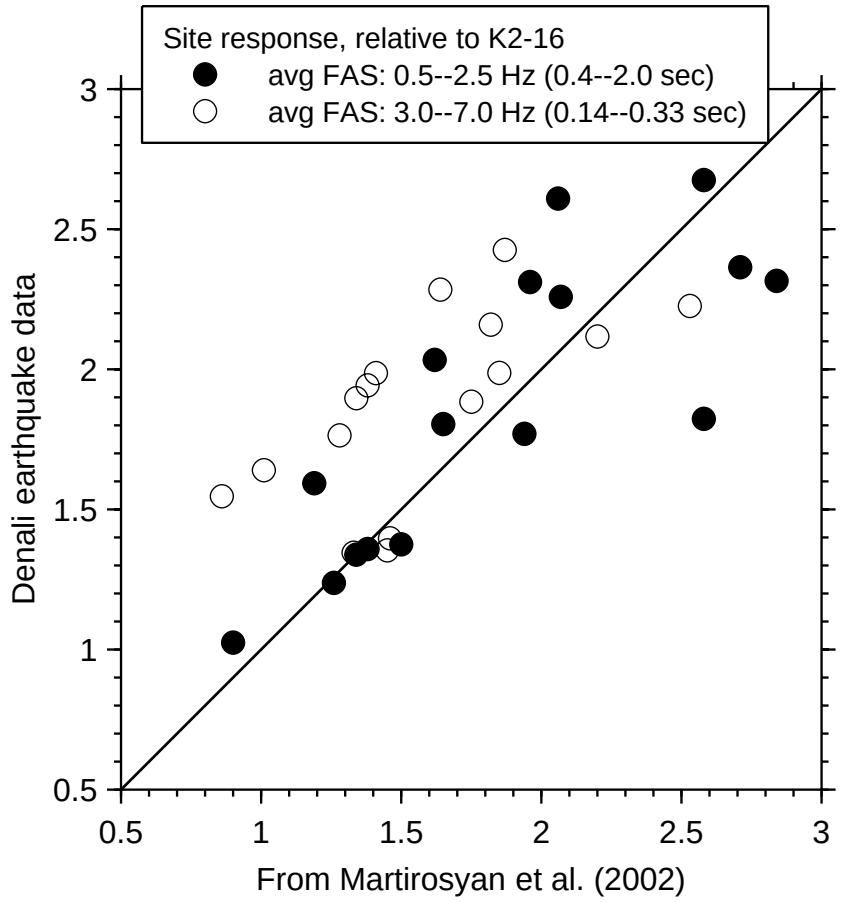

Figure 9. Comparison of site responses (relative to station K2-16) from smoothed Fourier amplitude spectra, as determined from the Denali earthquake data (EW component) and from Martirosyan *et al.* (2002; rms of the two horizontal components).

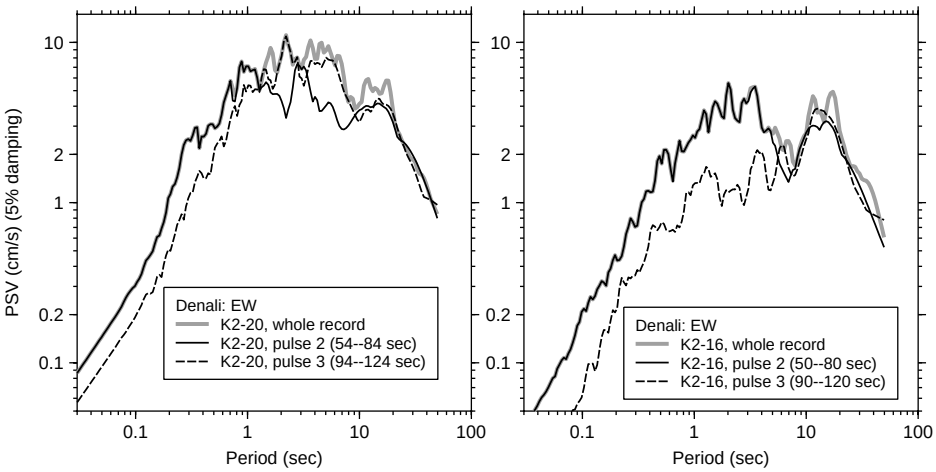

Figure 10. 5%-damped pseudo relative velocity response for the EW component at stations K2-20 and K2-16, from the whole record and from windows that include the two large displacement pulses (pulses 2 and 3 in Figure 2). The portions of the accelerograms have different influences on the response spectra. From the acceleration trace (Figure 4) it is clear that most of the energy at high frequencies is carried in the second pulse, so the response spectra from that pulse is essentially equal to the whole record response spectrum at shorter periods. Conversely, for this record the second and third pulses contribute about equally to the longer period response.

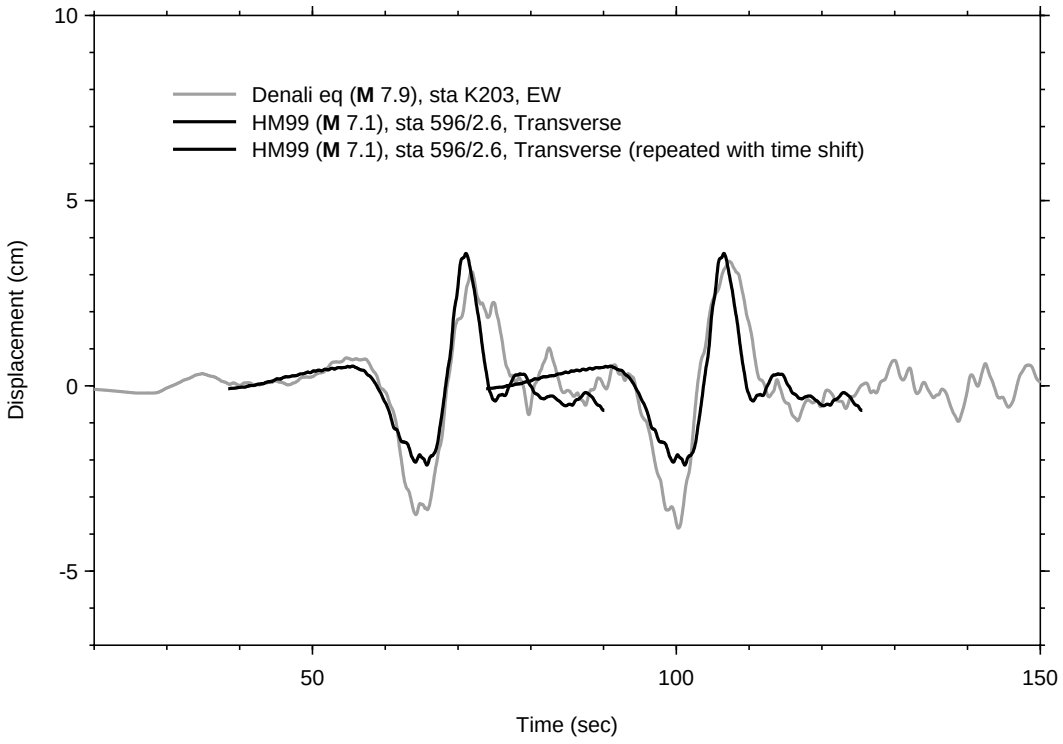

Figure 11. EW displacements from station K2-03 from the Denali earthquake. Superimposed are two copies, shifted in time, of the transverse displacements from the 596 recording of the Hector Mine (HM) earthquake. The HM motions have been divided by 2.6 to correct for the different distances to the earthquakes. The factor of 2.6 came from the ground-motion prediction equations of Sadigh *et al.* (1997). All records were low-cut filtered with a low-order acausal Butterworth filter with a corner at 0.02 Hz.

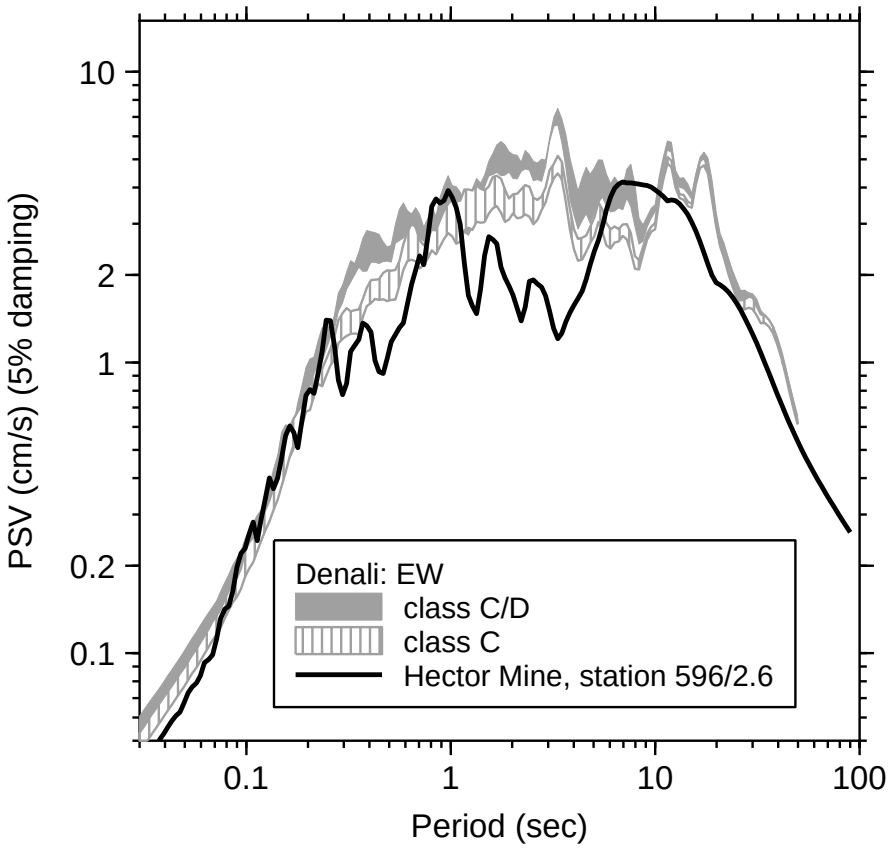

Figure 12. Response spectra for the Denali recordings and for the transverse component of the 1999 Hector Mine, California, earthquake (after dividing the HM spectrum by 2.6 to correct for the different distances to the earthquakes). All records were low-cut filtered with a low-order acausal Butterworth filter with a corner at 0.02 Hz.